Contribution from the Laboratoire de Synthèse et d'Electrosynthèse Organométallique associé au CNRS (UA 33), Faculté des Sciences "Gabriel", Université de Dijon, 6, Boulevard Gabriel, 21100 Dijon, France, Laboratoire de Chimie du Solide Minéral associé au CNRS (UA 158), Service de Chimie Minérale, Université de Nancy 1, BP No. 239, 54506 Vandoeuvre les Nancy, France, Laboratoire de Minéralogie et Cristallographie (UA 809), Faculté des Sciences, Centre de 2ème Cycle, Université de Nancy, BP No. 239, 54506 Vandoeuvre les Nancy, France, and Laboratoire de Spectrochimie des Elément de Transition (UA 420), Université de Paris Sud, 91405 Orsay, France

Characteristic Properties of High- and Low-Spin-State Five-Coordinate σ-Bonded Aryl-, Alkyl-, and Perfluoroaryliron(III) Porphyrins: ^{1}H NMR, ESR, Mössbauer, and Magnetic Studies

A. Tabard,[1a] P. Cocolios,[1a,e] G. Lagrange,[1a,f] R. Gerardin,[1b] J. Hubsch,[1c] C. Lecomte,[1c] J. Zarembowitch,[1d] and R. Guilard*[1a]

Received June 3, 1987

The magnetic behavior of σ-alkyliron(III) (or σ-aryliron(III)) porphyrins is studied in solution and in solid state by various spectroscopic methods: ^{1}H NMR, ESR, and ^{57}Fe Mössbauer spectroscopies. Variable-temperature magnetic susceptibility measurements were also performed on these complexes. The iron(III) atom of these compounds is present in different spin states. These are high ($S = {}^5/_2$) or low spin ($S = {}^1/_2$) at room temperature. Several factors can affect the spin state, the major parameter being the nature of the axial ligand. The perfluoroaryl axial groups (C_6F_4H, C_6F_5) lead to complexes in a pure high-spin state whatever the temperature. In contrast, the (P)Fe[R(Ar)] complexes where R = CH_3, Ar = C_6H_5 and *p*-MeC_6H_4, and P = OEP, TPP, T(*m*-Me)PP, T(*p*-Me)PP, T(*p*-Et_2N)PP, and (β-CN)$_4$TPP behave differently and are in a low-spin state at room temperature. However, for the latter compounds in frozen solution or in the solid state, some high-spin sites are observed by ESR spectroscopy. The amount is critically dependent on the nature of the axial and porphyrin ligands. Moreover, the solvent matrix appears very important. In the solid state and on the basis of ESR data, the spin mixture could be slightly modified by grinding of the crystalline sample, leading to high-spin entity increase. The effect of these parameters is examined with respect to the nature of the metal-porphyrin and metal-ligand bond. Correlations between stereochemistry, spin state, and the nature of ligands are discussed.

Introduction

In recent years, much research has been devoted to the study of various substrates occuring in catalytic processes of cytochrome P450. It was suggested that iron-carbon σ-bonded complexes could be formed upon the metabolic reduction of polyhalogenated compounds like carbon tetrachloride or halothane in the liver by cytochrome P450.[2-4] More recently, several studies have postulated that cytochrome P450, myoglobin, and hemoglobin give rise to intermediate σ-bonded iron(III) alkyl (or aryl) derivatives upon metabolic oxidation of various monosubstituted hydrazines.[5-9] Numerous synthetic models have been proposed to elucidate the formation of these intermediates.[10-19]

The physicochemical data of these σ-bonded complexes showed that their structural and electronic properties are very unusual in the iron porphyrin series. In most cases, these derivatives are described as low-spin pentacoordinated species[20-35] in contrast to other previously reported Fe(III) pentacoordinated compounds.[36,37] We have noted some abnormal behavior regarding the magnetic properties of these iron-carbon σ-bonded porphyrins. In this paper, we show that the iron atom is present in different spin states. These are high spin ($S = {}^5/_2$), low spin ($S = {}^1/_2$), or a mixture of high and low spin. Several factors govern the spin state of the iron center: the nature of the axial and equatorial ligand, the solvent, the temperature, and the method of sample preparation. In order to characterize the electronic properties of these σ-bonded iron porphyrins, their magnetic behavior has been investigated in solution and in the solid state. This present study shows the

(1) (a) Université de Dijon. (b) Service de Chimie Minérale, Université de Nancy. (c) Centre de 2ème Cycle, Université de Nancy. (d) Université de Paris Sud. (e) Present address: L'Air Liquide, CRCD, F 78350 Jouy en Josas, France. (f) Present address: LCC CICE, 21000 Dijon, France.
(2) Uehleke, H.; Hellmer, K. H.; Tabarelli-Poplawski, S. *Naunyn-Schmiedeberg's Arch. Pharmacol.* **1973**, *279*, 39.
(3) Mansuy, D.; Nastainczyk, W.; Ullrich, V. *Naunyn-Schmiedeberg's Arch. Pharmacol.* **1974**, *285*, 315.
(4) Wolf, C. R.; Mansuy, D.; Nastainczyk, W.; Deutschmann, G.; Ullrich, V. *Mol. Pharmacol.* **1977**, *13*, 698.
(5) Augusto, O.; Kunze, K. L.; Ortiz de Montellano, P. R. *J. Biol. Chem.* **1982**, *257*, 6231.
(6) Ortiz de Montellano, P. R.; Kunze, K. L. *J. Am. Chem. Soc.* **1981**, *103*, 6534.
(7) Kunze, K. L.; Ortiz de Montellano, P. R. *J. Am. Chem. Soc.* **1983**, *105*, 1380.
(8) Ortiz de Montellano, P. R.; Kerr, D. E. *Biochemistry* **1985**, *24*, 1147.
(9) Ringe, D.; Petsko, G. A.; Kerr, D. E.; Ortiz de Montellano, P. R. *Biochemistry* **1984**, *23*, 2.
(10) Mansuy, D. *Pure Appl. Chem.* **1980**, *52*, 698.
(11) Mansuy, D.; Chottard, J. C.; Lange, M.; Battioni, J. P. *J. Mol. Catal.* **1980**, *7*, 215.
(12) Mansuy, D.; Guerin, P.; Chottard, J. C. *J. Organomet. Chem.* **1979**, *171*, 195.
(13) Guerin, P.; Battioni, J. P.; Chottard, J. C.; Mansuy, D. *J. Organometal. Chem.* **1981**, *218*, 201.
(14) Brault, D.; Bizet, C.; Morlière, P.; Rougee, M.; Land, E. J.; Santus, R.; Swallow, A. J. *J. Am. Chem. Soc.* **1980**, *102*, 1015.
(15) Mansuy, D. *Rev. Biochem. Toxicol.* **1981**, *3*, 283.
(16) Brault, D.; Neta, P. *J. Am. Chem. Soc.* **1981**, *103*, 2705.
(17) Mansuy, D.; Fontecave, M.; Battioni, J. P. *J. Chem. Soc., Chem. Commun.* **1982**, 317.
(18) Mansuy, D.; Battioni, J. P. *J. Chem. Soc., Chem. Commun.* **1982**, 638.
(19) Brault, D.; Neta, P. *J. Phys. Chem.* **1982**, *86*, 3405.
(20) Reed, C. A.; Mashiko, T.; Bentley, S. P.; Kastner, M. E.; Scheidt, W. R.; Spartalian, K.; Lang, G. *J. Am. Chem. Soc.* **1979**, *101*, 2948.
(21) Lexa, D.; Saveant, J. M.; Battioni, J. P.; Lange, M.; Mansuy, D. *Angew. Chem., Int. Ed. Engl.* **1981**, *20*, 578.
(22) Clarke, D. A.; Dolphin, D.; Grigg, R.; Johnson, A. W.; Pinnock, H. A. *J. Chem. Soc. C* **1968**, 881.
(23) Lexa, D.; Mispelter, J.; Saveant, J. M. *J. Am. Chem. Soc.* **1981**, *103*, 6806.
(24) Ortiz de Montellano, P. R.; Kunze, K. L.; Augusto, O. *J. Am. Chem. Soc.* **1982**, *104*, 3545.
(25) Lexa, D.; Saveant, J. M. *J. Am. Chem. Soc.* **1982**, *104*, 3503.
(26) Ogoshi, H.; Sugimoto, H.; Yoshida, Z. I.; Kobayashi, H.; Sakai, H.; Maeda, Y. *J. Organomet. Chem.* **1982**, *234*, 185.
(27) Mansuy, D.; Battioni, J. P.; Duprê, D.; Sartori, E. *J. Am. Chem. Soc.* **1982**, *104*, 6159.
(28) Kunze, K. L.; Ortiz de Montellano, P. R. *J. Am. Chem. Soc.* **1983**, *105*, 1380.
(29) Battioni, P.; Mahy, J. P.; Gillet, G.; Mansuy, D. *J. Am. Chem. Soc.* **1983**, *105*, 1399.
(30) Cocolios, P.; Laviron, E.; Guilard, R. *J. Organomet. Chem.* **1982**, *228*, C 39.
(31) Cocolios, P.; Lagrange, G.; Guilard, R. *J. Organomet. Chem.* **1983**, *253*, 65.
(32) Lançon, D.; Cocolios, P.; Guilard, R.; Kadish, K. M. *J. Am. Chem. Soc.* **1984**, *106*, 4472.
(33) Lançon, D.; Cocolios, P.; Guilard, R.; Kadish, K. M. *Organometallics* **1984**, *3*, 1164.
(34) Doppelt, P. *Inorg. Chem.* **1984**, *23*, 4009.
(35) Balch, A. L.; Renner, M. W. *Inorg. Chem.* **1986**, *25*, 303.
(36) Scheidt, W. R.; Reed, C. A. *Chem. Rev.* **1981**, *81*, 543.
(37) Scheidt, W. R.; Gouterman, M. In *Iron Porphyrins*; Lever, A. B. P., Gray, H. B., Eds.; Addison-Wesley: Reading, MA, 1983; Part I, Chapter 2.

0020-1669/88/1327-0110$01.50/0

Table I. Porphyrin Proton Isotropic Shifts[a] of (P)Fe[R(Ar)] Complexes and Their Separation into Dipolar and Contact Contributions

compd	proton type	$(\Delta H/H)_{iso}$, ppm	$(\Delta H/H)_{dip}$, ppm	$(\Delta H/H)_{con}$, ppm
(OEP)Fe(*n*-C_4H_9)	meso-H	−6.62	−14.05	7.43
	α-CH_2	−1.81	−4.77	2.96
	α′-CH_2	−5.84	−4.77	−1.07
	β-CH_3	−4.07	−3.14	−0.93
(OEP)Fe(CH_3)	meso-H	−6.87	−14.58	7.71
	α-CH_2	−1.71	−4.95	3.24
	α′-CH_2	−6.27	−4.95	−1.32
	β-CH_3	−4.20	−3.25	−0.95
(OEP)Fe(C_6H_5)	meso-H	−4.68	−10.58	5.90
	α-CH_2	0.32	−3.59	3.91
	α′-CH_2	−5.84	−3.59	−2.25
	β-CH_3	−3.67	−2.36	−1.31
(OEP)-Fe(*p*-MeC_6H_4)	meso-H	−4.36	−9.68	5.32
	α-CH_2	0.28	−3.28	3.56
	α′-CH_2	−5.56	−3.28	−2.28
	β-CH_3	−3.53	−2.16	−1.37
(TPP)Fe(*n*-C_4H_9)	*o*-H	−4.53	−4.53	0.00
	o′-H	−5.80	−4.53	−1.27
	m-H	−3.51	−2.09	−1.42
	p-H	−2.45	−1.86	−0.59
	pyrr-H	−27.35	−8.54	−18.81
(TPP)Fe(CH_3)	*o*-H	−4.70	−4.70	0.00
	o′-H	−5.82	−4.70	−1.12
	m-H	−3.44	−2.17	−1.27
	p-H	−2.47	−1.93	−0.54
	pyrr-H	−28.15	−8.87	−19.29
(TPP)Fe(C_6H_5)	*o*-H	−3.41	−3.41	0.00
	o′-H	−5.45	−3.41	−2.04
	m-H	−3.35	−1.58	−1.77
	p-H	−2.20	−1.40	−0.80
	pyrr-H	−26.61	−6.43	−20.18
(TPP)-Fe(*p*-MeC_6H_4)	*o*-H	−3.12	−3.12	0.00
	o′-H	−5.08	−3.12	−1.96
	m-H	−3.05	−1.44	−1.61
	p-H	−1.92	−1.28	−0.64
	pyrr-H	−25.89	−5.89	−20.00
[T(*p*-Et_2N)PP]-Fe(C_6H_5)	*o*-H	−3.40	−3.40	0.00
	o′-H	−5.16	−3.40	−1.76
	m-H	−2.68	−1.57	−1.11
	pyrr-H	−25.69	−6.41	−19.28
[(β-$CN)_4$TPP]-Fe(C_6H_5)	*o*-H	−2.58	−2.58	0.00
	o′-H	−4.32	−2.58	−1.74
	m-H	−2.58	−1.19	−1.39
	m′-H	−3.14	−1.19	−1.95
	p-H	−1.93	−1.06	−0.87
	pyrr-H	−28.54	−4.87	−23.67

[a] In C_6D_6 solution at 21 °C.

correlation between the stereochemistry, the spin state, and the nature of the axial ligands in the iron porphyrin series.

Experimental Section

Synthesis. The synthesis of the σ-alkyliron (or σ-aryliron) porphyrins and the sample preparation were carried out under an argon atmosphere. All common solvents were thoroughly dried and were distilled under argon prior to use. All operations were carried out in Schlenk tubes. The following halogenated iron porphyrins[38] were prepared by literature methods: (OEP)FeCl,[39] (TPP)FeCl,[39] [T(*m*-Me)PP]FeCl,[39] [T(*p*-Me)PP]FeCl,[39] [T(*p*-Et_2N)PP]FeCl,[40] [(β-$CN)_4$TPP]FeCl.[41] Magnesium sulfate (Aldrich) was used without particular purification. The (perfluoroaryl)-, aryl-, and alkylferriporphyrins, (P)Fe[R(Ar)][31] were prepared by the action of an organomagnesium compound on the corresponding (porphyrinato)iron(III) chloride; detailed syntheses have been published elsewhere.[31,42]

Instrumentation. ^1H NMR spectra were recorded on a JEOL FX 100 or Bruker WM 400 instrument of the CEREMA ("Centre de Résonance Magnétique" of the University of Dijon). Spectra were measured from complex (5 mg) solutions in 0.6 cm^3 of C_6D_6 or $C_6D_5CD_3$ with tetramethylsilane as internal reference. When carbon disulfide was used as solvent, a toluene-d_8 capillary was introduced in NMR cells. The temperatures are given within 0.7 K.

ESR spectra were recorded at 115 K in frozen solution ($[Fe^{III}] \simeq 0.02$ M) (toluene, carbon disulfide) or in the solid state (7% dilution in magnesium sulfate) with a Varian E4-X band spectrometer equipped with a nitrogen low-temperature device. The *g* values were measured with respect to diphenylpicrylhydrazyl ($g = 2.0036 \pm 0.0003$). Complementary ESR measurements down to helium temperature were made with a Bruker ER 200 D-X band spectrometer equipped with an Oxford ESR 900 cryostat (Laboratoire de Spectrochimie des Elements de Transition).

Mössbauer measurements were carried out with Elscint AME 40C and Halder spectrometers with constant acceleration and recorded on 1024 channels with folding in line. Each calculated spectrum was refined by a least-squares method with Lorentzian line shapes (Laboratoire de Chimie du Solide Minéral).

Magnetic measurements were obtained on a SHE SQUID magnetometer with 50-mg solid samples under a 10-KOe magnetic field (Laboratoire de Minéralogie et Cristallographie).

Table II. Separation of the Isotropic Shifts into Contact and Dipolar Contributions[a] for the Axial Ligands of (P)Fe(Ar) Complexes

compd	proton type	$(\Delta H/H)_{iso}$, ppm	$(\Delta H/H)_{dip}$, ppm	$(\Delta H/H)_{con}$, ppm
(OEP)Fe(C_6H_5)	*o*-H	−82.61	20.46	−103.07
	m-H	7.72	10.91	−3.19
	p-H	−29.64	9.89	−39.53
(OEP)Fe(*p*-MeC_6H_4)	*o*-H	−85.76	18.72	−104.48
	m-H	9.69	9.98	−0.29
	p-CH_3	59.06	5.62	53.44
(TPP)Fe(C_6H_5)	*o*-H	−83.97	20.46	−104.43
	m-H	7.85	10.91	−3.06
	p-H	−32.99	9.89	−42.88
(TPP)Fe(*p*-MeC_6H_4)	*o*-H	−88.88	18.72	−107.60
	m-H	9.98	9.98	0.00
	p-CH_3	63.69	5.62	58.07
[T(*p*-Et_2N)PP]-Fe(C_6H_5)	*o*-H	−81.80	20.40	−102.20
	m-H	7.85	10.88	−3.03
	p-H	−30.45	9.86	−40.31
[(β-$CN)_4$TPP]-Fe(C_6H_5)	*o*-H	−91.39	15.48	−106.87
	m-H	6.82	8.26	−2.44
	p-H	−47.11	7.48	−54.59

[a] Relative geometric factors $(3\cos^2\theta - 1)r^{-3}$ from La Mar et al. (La Mar, G. N.; Bold, T. J.; Satterlee, J. D. *Biochim. Biophys. Acta* **1977**, *498*, 189) and calculated from ref 34.

Table III. Proton Isotropic Shifts[a] of the High-Spin Fe(III) Complexes (P)FeCl, (P)Fe(C_6F_5), and (P)Fe(C_6F_4H)

proton type	OEP			TPP		
	Cl	C_6F_5	C_6F_4H	Cl	C_6F_5	C_6F_4H
			Porphyrin			
α-CH_2	35.52	38.66	38.88			
α′-CH_2	35.52	37.68	35.90			
β-CH_3	4.28	4.32	4.03			
meso-H	−66.70	−65.53	−59.06			
c-H				0.05	0.09	−0.23
o′-H				−2.90	−2.76	−2.74
m-H				5.31	4.02	3.61
m′-H				3.68	3.21	2.87
p-H				−1.31	−1.31	−1.26
pyrr-H				72.59	57.16	52.08
			Axial Ligand			
p-H			−63.55			−66.43

[a] Shifts given in ppm, at 21 °C; solvent = C_6D_6.

(38) Abbreviations used: P, any porphyrin; $(OEP)H_2$, octaethylporphyrin; $(TPP)H_2$, tetraphenylporphyrin; $[T(m\text{-}Me)PP]H_2$, tetrakis(*m*-methylphenyl)porphyrin; $[T(p\text{-}Me)PP]H_2$, tetrakis(*p*-methylphenyl)porphyrin; $[T(p\text{-}Et_2N)PP]H_2$, tetrakis(*p*-(diethylamino)phenyl)porphyrin; $[(\beta\text{-}CN)_4TPP]H_2$, tetracyanotetraphenylporphyrin; $(TAP)H_2$, tetrakis(*p*-methoxyphenyl)porphyrin.

(39) Buchler, J. W. In *The Porphyrins*; Dolphin, D., Ed.; Academic: New York, 1978; Vol. I, Chapter 10.

(40) Walker, F. A.; Balke, V. L.; McDermott, G. A. *J. Am. Chem. Soc.* **1982**, *104*, 1569.

(41) Giraudeau, A.; Callot, H. J.; Jordan, J.; Ezhar, I.; Gross, M. *J. Am. Chem. Soc.* **1979**, *101*, 3857.

(42) Guilard, R.; Boisselier-Cocolios, B.; Tabard, A.; Cocolios, P.; Simonet, B.; Kadish, K. M. *Inorg. Chem.* **1985**, *24*, 2509.

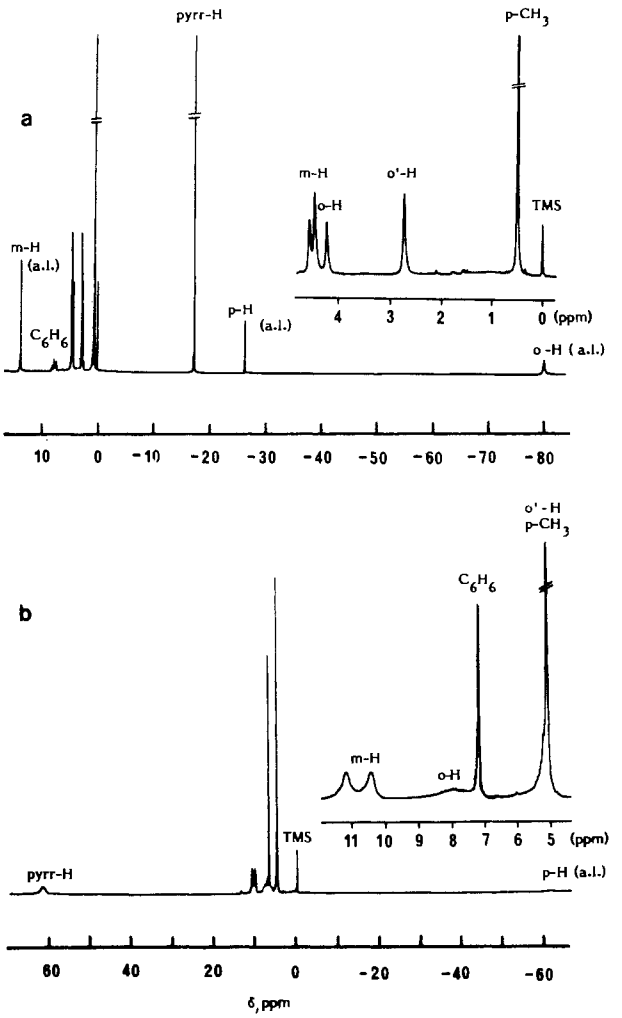

Figure 1. ^{1}H NMR spectra of (a) [T(*p*-Me)PP]Fe(C_6H_5) and (b) [T-(*p*-Me)PP]Fe(C_6F_4H) recorded at 294 K in C_6D_6.

Results

^{1}H NMR. The proton NMR traces of [T(*p*-Me)PP]Fe(C_6H_5) and [T(*p*-Me)PP]Fe(C_6F_4H) in C_6D_6 are shown in Figure 1, and Tables I–III summarize the isotropic chemical shifts for the (P)Fe[R(Ar)] derivatives in hexadeuteriobenzene. The isotropic chemical shifts have been calculated by using diamagnetic isostructural (P)In[R(Ar)] complexes as reference.[31,42-44]

Two kinds of spectra are obtained in C_6D_6 at 294 K. Complexes with an alkyl or aryl axial ligand (CH_3, *n*-C_4H_9, C_6H_5, *p*-MeC_6H_4) have pyrrole proton resonances between −25.69 and −28.54 ppm for tetraaryl–porphyrin macrocycles, and the meso protons give signals in the range −4.36 to −6.87 ppm for octaethylporphyrin macrocycles (see Table I). These spectra are typical of an iron(III) in a low-spin state.[45] On the contrary, complexes with perfluoro axial ligands (C_6F_4H, C_6F_5) give rise to characteristic signals of an high-spin species.[45] The pyrrole protons of tetraarylporphyrins are located between 52.08 and 57.16 ppm whereas the meso protons of octaethylporphyrins appear in the region −59.06 to −65.53 ppm (see Table III).

In order to characterize the alkyliron (or aryliron) porphyrin's electronic structure, analysis of the chemical shifts was made according to the method of La Mar and Walker.[45] The axial geometric factor calculated values of the different porphyrin proton sites of (TPP)Fe$(Im)_2^+Cl^-$ and (TPP)Fe(C_6H_5) were used to determine the corresponding dipolar shifts. The results are summarized in Tables I and II.

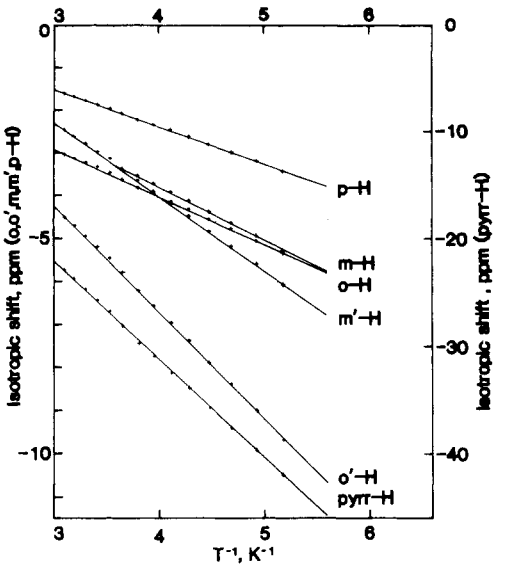

Figure 2. Curie plot for (TPP)Fe(*p*-MeC_6H_4) in toluene-d_8.

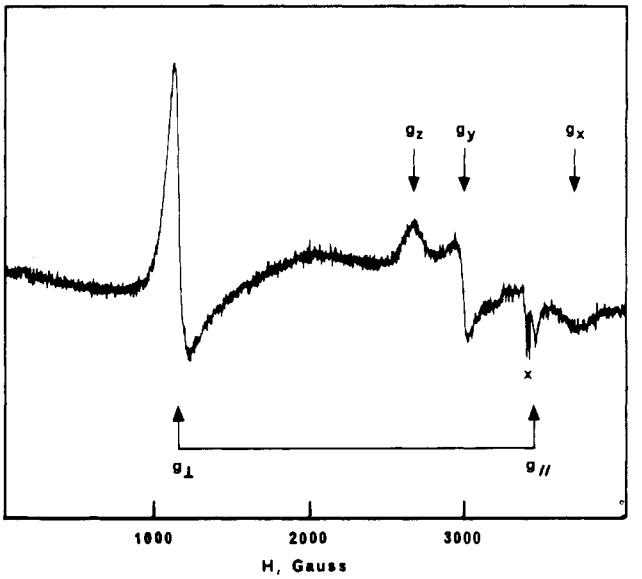

Figure 3. X-Band ESR spectrum of [T(*p*-Me)PP]Fe(C_6H_5) recorded at 115 K in toluene (microwave frequency = 9.60 GHz, microwave power = 63 mW, X = free-radical signal).

Also, analysis of the curve in the Curie plot was made for the same complexes. As example, a plot of the shift data for various resonances of (TPP)Fe(*p*-MeC_6H_4) in toluene-d_8 versus T^{-1} is shown in Figure 2. There is a linear dependence on T^{-1} in the range 193–333 K. This linearity agrees with an iron(III) center in a low-spin state ($S = {}^1/_2$) for all complexes with a coordinated alkyl or aryl axial ligand.

ESR. The *g* values of all the complexes in toluene at 115 K are summarized in Table IV. For the low-spin state, the higher values of g_z and the products of the three values are supposed to be positive.[46] The calculations of the rhombic (V/λ) and tetragonal (Δ/λ) distortions (in units of the spin–orbit constant) are made from the following equations:[47]

$$\frac{V}{\lambda} = \frac{g_x}{g_z + g_y} + \frac{g_y}{g_z - g_x}$$

$$\frac{\Delta}{\lambda} = \frac{g_x}{g_z + g_y} + \frac{g_z}{g_y - g_z} - \frac{V}{2\lambda}$$

(43) Cocolios, P.; Guilard, R.; Fournari, P. *J. Organomet. Chem.* **1979**, *179*, 311.
(44) Tabard, A.; Guilard, R.; Kadish, K. M. *Inorg. Chem.* **1986**, *25*, 4277.
(45) La Mar, G. N.; Walker, F. A. In *The Porphyrins*; Dolphin, D., Ed.; Academic: New York, 1979; Vol. IV, Chapter 2.
(46) Palmer, G. In *The Porphyrins*; Dolphin, D., Ed.; Academic: New York, 1979; Vol. IV, Chapter 6.

Table IV. ESR Data of the Investigated (P)Fe[R(Ar)] in Toluene at 115 K

compd	$S = {}^1/_2$						$S = {}^5/_2$	
	g_x	g_y	g_z	Δ/λ	V/λ	V/Δ	$g_\perp$	$g_\parallel$
(OEP)Fe(n-C_4H_9)							5.99	1.99
(OEP)Fe(CH_3)							6.17	2.01
(OEP)Fe(C_6H_5)							6.31	1.99
(OEP)Fe(p-MeC_6H_4)							5.99	2.02
(TPP)Fe(n-C_4H_9)	1.90	2.28	2.56	5.20	3.85	0.74	6.10	1.98
(TPP)Fe(CH_3)	1.89	2.27	2.60	5.44	3.56	0.65	6.08	
(TPP)Fe(C_6H_5)	1.92	2.39	2.60	4.14	3.51	0.85	5.96	
(TPP)Fe(p-MeC_6H_4)	1.86	2.23	2.48	5.98	3.99	0.67	5.97	
[T(m-Me)PP]Fe(n-C_4H_9)	1.89	2.27	2.52	5.03	3.99	0.79	6.45	1.99
[T(m-Me)PP]Fe(CH_3)	1.87	2.28	2.61	5.02	3.46	0.69	6.02	1.99
[T(m-Me)PP]Fe(C_6H_5)	1.86	2.25	2.55	5.11	3.65	0.71	6.02	1.98
[T(p-Me)PP]Fe(n-C_4H_9)	1.88	2.27	2.53	4.94	3.88	0.78	6.26	1.98
[T(p-Me)PP]Fe(CH_3)	1.88	2.30	2.57	4.65	3.72	0.80	6.08	
[T(p-Me)PP]Fe(C_6H_5)	1.81	2.31	2.63	5.04	3.18	0.63	6.08	1.96
[T(p-Et_2N)PP]Fe(C_6H_5)							5.96	2.02
[(β-CN)$_4$TPP]Fe(C_6H_5)	1.97	2.06	2.25	21.55	7.81	0.36		
(OEP)Fe(C_6F_4H)							5.88	1.98
(OEP)Fe(C_6F_5)							6.08[a]	1.97[a]
(TPP)Fe(C_6F_4H)							5.86	1.98
(TPP)Fe(C_6F_5)							5.86	1.99
[T(m-Me)PP]Fe(C_6F_4H)							5.86	1.98
[T(m-Me)PP]Fe(C_6F_5)							5.86	1.98
[T(p-Me)PP]Fe(C_6F_4H)							5.81	1.98
[T(p-Me)PP]Fe(C_6F_5)							5.85	1.98

[a] In 2:1 toluene–methylene chloride mixtures.

Table V. ESR Data of the Investigated (P)Fe[R(Ar)] in Carbon Disulfide at 115 K

compd	$S = {}^1/_2$						$S = {}^5/_2$	
	g_x	g_y	g_z	Δ/λ	V/λ	V/Δ	$g_\perp$	$g_\parallel$
(OEP)Fe(CH_3)	1.93	2.26	2.48	5.66	4.52	0.80		
(OEP)Fe(C_6H_5)	1.81	2.04	2.31	8.21	4.50	0.55	5.87	
(TPP)Fe(CH_3)	1.88	2.27	2.61	5.33	3.49	0.66		
(TPP)Fe(C_6H_5)	1.85	2.30	2.58	4.35	3.53	0.81	5.93	

These calculations lead to the rhombic character (V/Δ) of the studied complexes.

A typical spectrum of a ferriporphyrin derivative ([T(p-Me)PP]Fe(C_6H_5)) in toluene at 115 K is reproduced in Figure 3. The characteristic signals of a low-spin complex (g_x, g_y, g_z) are observed in the range 2500–3500 G together with two signals ($g_\perp \simeq 6$, $g_\parallel \simeq 2$) attributable to a high-spin complex ($S = {}^5/_2$). Such a spectrum was not observed for each complex (see Table IV). The above results lead to a contradiction: for certain complexes, the ^{1}H NMR data are in accordance with low-spin Fe(III) whereas the ESR data are typical of a high-spin species, the solvent being benzene or toluene. In order to understand this different behavior, we have studied the dependence of ESR spectra on temperature. Figure 4 reproduces the variation of the product of the microwave absorption intensity and temperature (IT) versus T for (OEP)Fe(C_6H_5) in toluene. This was done for the $g_\perp$ and $g_\parallel$ signals, I being the corrected intensity.[48] Indeed, it was shown that IT is proportional to χT, where χ is the magnetic susceptibility of the entity at T.[49] These curves show clearly the evolution of the two signals: the $g_\perp$ signal decreases very quickly in the range 0–50 K and then is constant at higher temperature whereas the curve of the second signal has a positive and regular slope. It was checked that the ESR signals did not saturate at the microwave power used ($\simeq$35 mW). Thus no iron spin state change is observed in frozen toluene solution when the temperature increases. However, in contrast to NMR results, the high-spin state is observed with some (alkyl or aryl)ferriporphyrins (see Table IV).

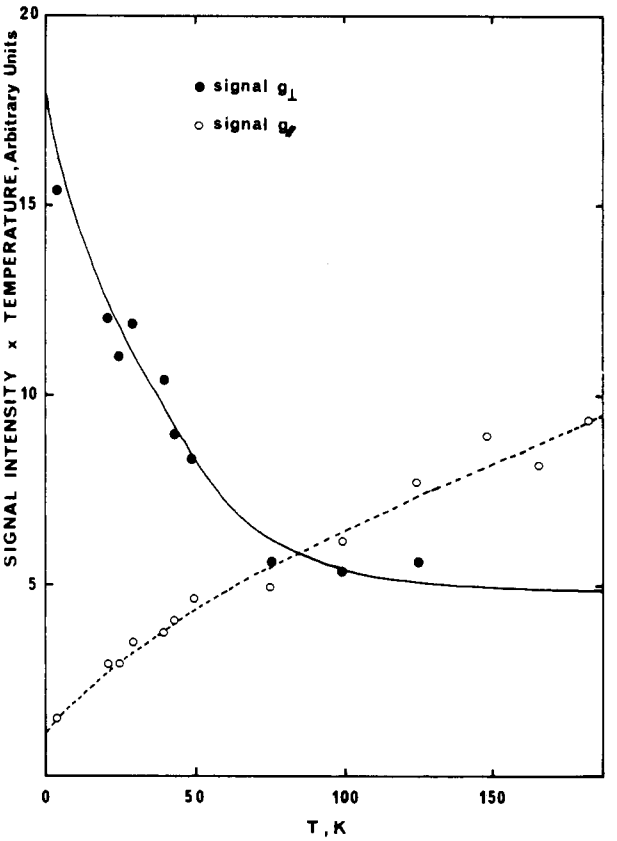

Figure 4. Plot of IT vs T for (OEP)Fe(C_6H_5) in Toluene.

Furthermore, the effect of various physical parameters was investigated. The ESR spectra were recorded in different solvents, which led to very interesting results. The g values of different complexes in carbon disulfide solution at 115 K are given in Table V. Figure 5 compares the two spectra of (OEP)Fe(CH_3) in toluene and in carbon disulfide at 115 K. In CS_2, we note a remarkable change. The characteristic signals of the high-spin entity disappear, and only the absorptions of the low-spin species are observed. This behavior does not occur in all cases. When the axial ligand is a methyl group, the transformation from a

(47) Palmer, G. In *Iron Porphyrins*; Lever, A. B. P., Gray, H. B., Eds.; Addison-Wesley: Reading, MA, 1983; Part II, Chapter 2.
(48) Wertz, J. E.; Bolton, J. R. *Electron Spin Resonance*; McGraw-Hill: New York, 1972; Chapter 2.
(49) Abragam, A.; Bleaney, B. *EPR of Transition Ions*; Clarendon: Oxford, England, 1970.

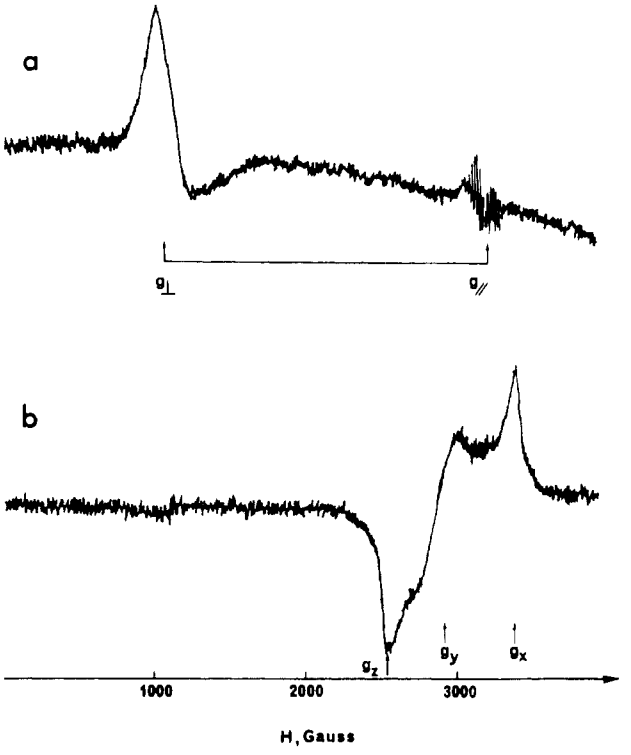

Figure 5. X-Band ESR spectra of (OEP)Fe(CH_3) recorded at 115 K (a) in toluene and (b) in carbon disulfide.

Table VI. ESR Data of the Investigated (P)Fe[R(Ar)] in Magnesium Sulfate with Grinding at 115 K

	$S = {}^1/_2$						$S = {}^5/_2$	
compd	g_x	g_y	g_z	Δ/λ	V/λ	V/Δ	$g_\perp$	$g_\parallel$
(OEP)Fe(CH_3)							6.16	1.99
(OEP)Fe(C_6H_5)							6.13	2.02
(TPP)Fe(CH_3)	1.90	2.30	2.64	5.24	3.49	0.67	5.93	
(TPP)Fe(C_6H_5)	1.89	2.29	2.52	4.68	4.03	0.86	5.95	2.02

high-spin state (or HS + LS) to a pure low-spin state at 115 K is observed. For the aryl derivatives (C_6H_5, p-MeC_6H_4) the change is incomplete, especially in the case of octaethylporphyrins. On the contrary, no solvent effect occurs for the perfluoro derivatives.

These results demonstrate that the spin states of (alkyl or aryl)ferriporphyrins are critically solvent dependent and led us to study these complexes in solid state. Figure 6a reproduces the ESR crystalline spectrum of nonground (TPP)Fe(CH_3) diluted in $MgSO_4$ (7%) at 6 K. The spectrum and the temperature dependence are similar to those observed in toluene frozen solution. All the complexes behave the same. Ground samples lead to different ESR spectra. The g values of various complexes with alkyl or aryl axial ligands are summarized in Table VI, and Figure 6b gives the spectrum of ground (TPP)Fe(CH_3) at 6 K. The intensity of the high-spin signals increases, and that of the low-spin signals decreases. These results indicate that the relative proportions of the two spin states are dependent on the method of sample preparation. No concentration effect has been shown in the solid state. In addition an isotropic superhyperfine coupling of about 16 G appears close to the 3250-G region and disappears at very low temperature and is essentially observed for the complexes in a low-spin state. Such hyperfine interaction has never been observed for the aryl derivatives of tetraphenylporphyrins (TPP)Fe(C_6H_5) or (TPP)Fe(p-MeC_6H_4)), which exhibit a very weak low spin signal. In the case of alkyliron(III) tetraphenylporphyrin derivatives (see Figure 6), the intensity of the superhyperfine lines depends on the grinding and decreases with a decreasing of the low-spin signal. For octaethylporphyrin compounds, a coupling is only observed in the case of alkyl derivatives. The presence of a free-radical impurity cannot be totally excluded; however, the same coupling was always observed whatever the synthesis and the starting material. The origin of this superhyperfine splitting is not clear-cut. Indeed, it is too sharp to derive from the metal center, and the coupling constant ($\simeq$16 G) is not

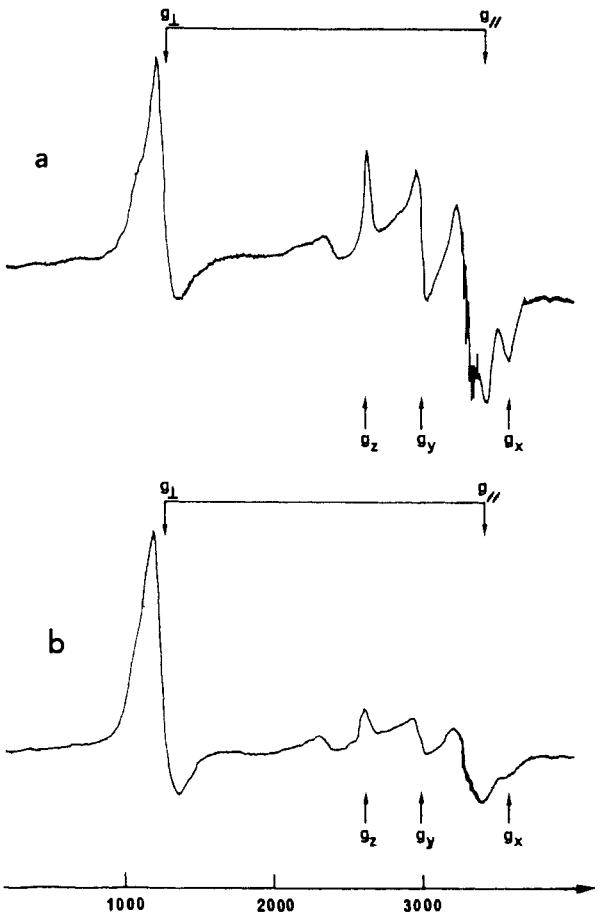

Figure 6. X-Band ESR spectra of (TPP)Fe(CH_3) recorded at 6 K in magnesium sulfate (7%) (a) without grinding and (b) with grinding.

Table VII. Mössbauer Data for (Porphyrinato)iron(III) Complexes

compd	T, K	δ,[a] mm s^{-1}	ΔE_Q, mm s^{-1}	spin state	ref
(TPP)FeCl	4.2	0.30	0.48	${}^5/_2$	60
(TPP)Fe(C_6F_4H)	85	0.53	0.48	${}^5/_2$	*e*
(OEP)Fe(C_6F_5)	178	$\simeq$0.22	...		*e*
	80	$\simeq$0.23	...		
hemoglobin azide	195	0.26	2.30	${}^1/_2$	63
hemoglobin cyanide	195	0.29	1.40	${}^1/_2$	63
(TPP)Fe(Im)$_2$Cl	298	0.13	2.11	${}^1/_2$	62
	77	0.23	2.23		
(OEP)Fe(CH_3)[b]	295	0.25	2.13	${}^1/_2$	*e*
	193	0.31	2.14		
	80	0.34	2.16		
[(OEP)Fe]$_2$O	80	0.40	0.76		*e*
(OEP)Fe(C_6H_5)	295	$\simeq$0.20	$\simeq$2.10	${}^1/_2$	*e*
	230	0.22	2.18		
	144	0.27	2.27		
	95	0.27	2.30		
(OEP)Fe(C_6H_5)[c]	295	0.20	2.16	${}^1/_2$	*e*
	143	0.26	2.28		
	85	0.28	2.30		
(OEP)Fe(C_6H_5)[d]	85	0.28	2.32	${}^1/_2$	*e*
(OEP)Fe(ClO_4)	295	0.29	3.16		61
	115	0.37	3.52		
	4.2	0.37	3.57		

[a] Relative to metallic iron. [b] [(OEP)Fe]$_2$O signals were observed. [c] In magnesium sulfate (1:1) without grinding. [d] In magnesium sulfate (1:1) with grinding. [e] This work. [f] Spin mixed with predominantly $S = {}^3/_2$ spin state.

Table VIII. Mössbauer Spectral Data for (OEP)Fe(C_6H_5) and (OEP)Fe(CH_3)

compd	T, K	δ,[a] mm s^{-1}	ΔE_Q, mm s^{-1}	Γ_-,[b] mm s^{-1}	Γ_+,[b] mm s^{-1}	I_-,[c] %	I_+,[c] %	χ_2[d]
(OEP)Fe(C_6H_5)	295[e]	≃0.20	≃2.10					
	230[e]	0.22	2.18	0.54	0.57	48.0	52.0	13.0
	144	0.27	2.27	0.39	0.40	49.5	50.5	1.4
	95	0.27	2.30	0.47	0.53	48.0	52.0	1.2
(OEP)Fe(C_6H_5)[f]	295[g]	0.20	2.16	0.24	0.24	51.0	49.0	1.1
	143	0.26	2.28	0.32	0.32	50.0	50.0	1.3
	85	0.28	2.30	0.32	0.41	49.5	50.5	1.5
(OEP)Fe(C_6H_5)[h]	85	0.28	2.32	0.27	0.34	51.0	49.0	1.1
(OEP)Fe(CH_3)	193	0.30	2.08	0.26	0.29	...	...	
	80	0.33	2.10	0.27	0.35	...	...	

[a] Relative to metallic iron. [b] Width of the lower energy line (Γ_-) and the higher energy line (Γ_+). [c] Proportion of each line calculated with the relative area. [d] Test of fit. [e] Spectra with weak resolution. [f] In magnesium sulfate (1:1) without grinding. [g] Well-resolved doublet with a high number of counts (≃9 × 10^6 counts/channel). [h] In magnesium sulfate (1:1) with grinding.

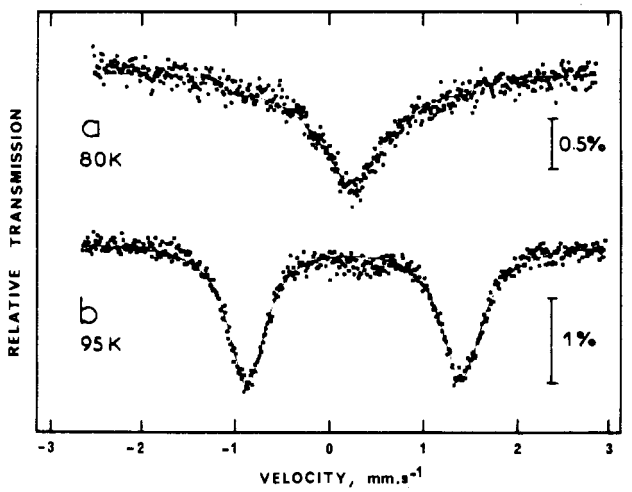

Figure 7. Mössbauer spectra of (a) (OEP)Fe(C_6F_5) (80 K) and (b) (OEP)Fe(C_6H_5) (95 K) in the solid state without grinding.

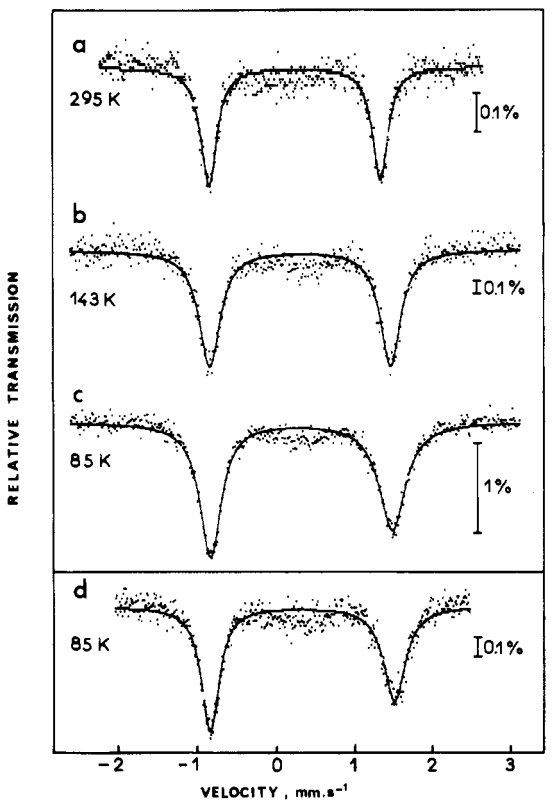

Figure 8. Mössbauer spectra of (OEP)Fe(C_6H_5) in magnesium sulfate (50%) without grinding at (a) 295 K, (b) 143 K, and (c) 85 K and (d) with Grinding at 85 K.

characteristic of a metal-free porphyrin radical; it might derive from nitrogen or hydrogen atoms.

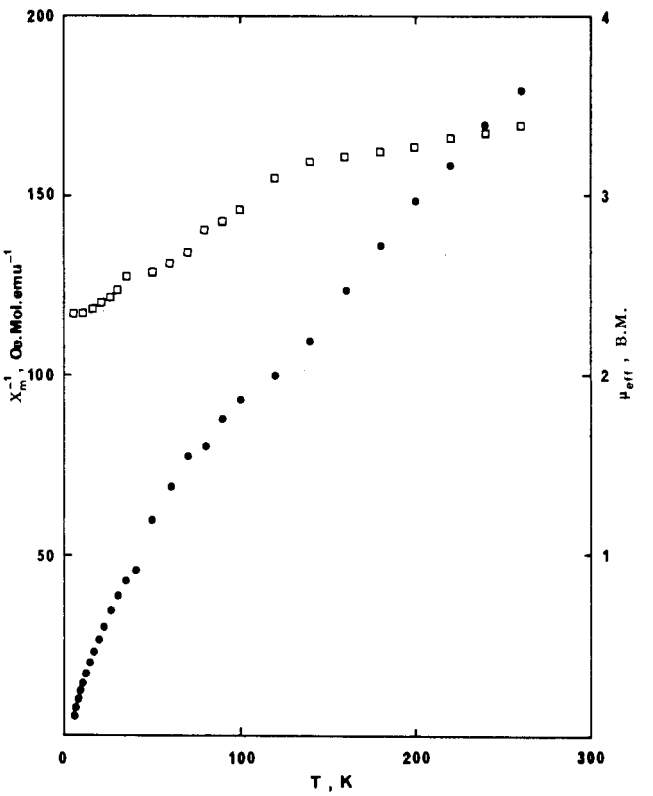

Figure 9. Plot of χ^{-1} vs T(●) and μ_B vs T(□) for (OEP)Fe(C_6H_5).

^{57}Fe Mössbauer Spectroscopy. On the basis of ESR data, it was of interest to complete the measurements in the solid state. Isomeric shifts (δ, mm s^{-1}) and quadrupolar splittings (ΔE_Q, mm s^{-1}) for several iron σ-bonded porphyrins are given in Table VII together with those observed for some iron(III) porphyrins with a well known spin state. Figure 7 shows the Mössbauer spectra of (OEP)Fe(C_6F_5) and (OEP)Fe(C_6H_5), and Figure 8 shows the Mössbauer spectra of (OEP)Fe(C_6H_5) in magnesium sulfate at several temperatures and with or without grinding. A clear difference is observed between the complexes with alkyl or aryl ligands and those with perfluoroaryl ligands (Table VII). The Mössbauer data of the former compounds are similar to those of low-spin derivatives whereas (perfluoroaryl)iron(III) porphyrin is clearly in a high-spin state ($S = {}^5/_2$) whatever the temperature. Furthermore, we have recorded the Mössbauer spectrum of (OEP)Fe(C_6H_5) diluted in magnesium sulfate with grinding for comparison with ESR data (Figure 8d). The characteristics of this latter spectrum are very close to those described above (Figure 8 and Table VII). Also Table VIII gives the Mössbauer parameters of (OEP)Fe(C_6H_5) for various sample preparations (diluted or not, with or without grinding); no significant difference is observed.

Magnetic Measurements. Measurements of variable temperature magnetic susceptibility on (OEP)Fe(C_6H_5) and (OEP)-Fe(CH_3) at a field strength of 10 000 G were performed on the

solid material between 5 and 270 K. The molar susceptibilities are corrected for the diamagnetism of the OEP ligand[50] and the axial ligand.[51] A plot of the inverse corrected molar susceptibilities vs temperature is given in Figure 9. All the observed data were corrected for the diamagnetism contribution of the sample holder. The effective magnetic moment of (OEP)Fe(C_6H_5) was calculated from

$$\mu_{eff} = 2.828(\chi T)^{1/2}$$

This value is plotted on Figure 9. Between 0 and 100 K the magnetic moment increases from 2.35 to 3.00 μ_B, and for the higher temperatures the slope of the curve decreases. The magnetic data on diluted (OEP)Fe(C_6H_5) in magnesium sulfate were recorded with and without grinding of the sample. No significant difference was observed. The obtained data are significantly higher than the magnetic moment of a pure low-spin state, which is close to 1.73 μ_B.

Discussion

Ferriporphyrinic systems show three spin states:[52] low-spin ($S = {}^1/_2$), intermediate-spin ($S = {}^3/_2$), and high-spin states ($S = {}^5/_2$). An admixed spin state ($S = {}^3/_2, S = {}^5/_2$) has also been observed. However, only a few derivatives show magnetic behavior, depending on various parameters, leading to a spin equilibrium[53] or a spin mixture.[54-56] (Alkyl or aryl)ferriporphyrins present a typical behavior. This is discussed below with respect to factors governing the spin state. These are the nature of the axial and equatorial ligands, the solvent, and the method of sample preparation.

Effect of the Nature of the Axial Ligand. When a perfluoroaryl group is coordinated to the iron metal, ^{1}H NMR and ESR spectra are characteristic of high-spin Fe(III) porphyrins whatever the nature of the porphyrin macrocycle. This is true at all temperatures in all solvents and for all sample preparations. This behavior is very close to that described for halogenoferriporphyrins. In particular, these perfluoroaryl σ-bonded derivatives have a C_{4v} symmetry, as clearly demonstrated by the splitting of the α-CH_2 and the ortho proton peaks in octaethylporphyrin and tetraphenylporphyrin complexes respectively (see Table III). The data summarized in Table III are in good agreement with σ spin density at the pyrrole positions and π spin density at the meso site, implying delocalization of unpaired electron spin from the d_{xz} and d_{yz} orbitals to the lowest vacant e-symmetry porphyrin orbitals, 4e(π^*). No dramatic change is observed between the C_6F_5 and C_6F_4H complexes. But, compared to those in the chloroiron porphyrins, pyrrole proton signals are at stronger field, implying that the σ-type spin density of the $d_{x^2-y^2}$ orbital is clearly related to the axial ligand nature[57] (see Table III). Also, we cannot exclude the possibility that some low-lying excited states of appropriate symmetry are spin-mixed with the $^6A_1$ ground state via spin–orbit coupling. The para proton of the C_6F_4H axial group gives a strong upfield resonance signal in the range −63.55 to −66.43 ppm according to the porphyrin macrocycle (Table III), this large upfield shift being due to the electron-withdrawing character of the perfluoro axial ligand, which induces a metal to axial ligand charge transfer.

The alkyl- or aryliron(III) porphyrins behave differently. The room-temperature NMR data are characteristic of low-spin-state ferriporphyrin systems although the pentacoordination scheme is usually associated with high-spin derivatives.[36] This unusual result can be attributed to the strong field character of the alkyl and aryl ligands. The calculation of contact and dipolar contributions to isotropic shifts according to the empirical method of La Mar and Walker[45] led us to determine the nature of the metal–porphyrin and metal–ligand bonding. In axial symmetry, the dipolar shift is given by the following equation,[45] where $(3\cos^2\theta - 1)r^{-3}$ is the geometric factor:

$$\left(\frac{\Delta H}{H}\right)_{dip} = \frac{1}{3N}(\chi_\parallel - \chi_\perp)\frac{3\cos^2\theta - 1}{r^3}$$

The relative dipolar shift for nonequivalent protons in a complex is solely given by the relative geometric factors. Indeed, no unpaired spin must be delocalized into meso aryl groups because the orientation of the meso aryl groups is nearly perpendicular to the porphyrin macrocycle.[35] All of the observed results are summarized in Tables I and II.

The large upfield pyrrole proton contact shifts and the small methylene (α-CH_2) proton contact shifts agree with charge transfer from the porphyrin 3e(π) orbitals to the d_{xz} and d_{yz} orbitals. This is expected for low-spin iron(III) derivatives. However, the large meso proton contact shifts indicate less polarization of the σ-electronic system induced by the porphyrin π ring current. This latter phenomenon increases with the inductive character of the axial ligand and demonstrates the critical dependence of the porphyrin electronic system on the nature of axial ligand.

The alternate sign of axial ortho, meta, and para proton isotropic shifts indicates a strong contact contribution induced by unpaired spin delocalization of the lowest π^* orbital of the axial aryl group. This is agreeable with the small meta proton contact shifts. Moreover, when the axial para proton is substituted by a methyl group, the contact shifts of these sites have similar magnitude but opposite signs. Thus, the coordination of an alkyl or aryl group to the metal center leads to low-spin iron(III) porphyrin derivatives with unpaired π-spin density on the aryl group, this charge transfer occuring from the occupied π-symmetry d_{xz} and d_{yz} orbitals.

Temperature dependence of the σ-bonded complex (TPP)Fe(p-MeC_6H_4) is illustrated in Figure 2. All of the porphyrin proton isotropic shifts follow the Curie law in the temperature range 193–333 K, and the nonzero temperature intercept can be due in part to dipolar interactions, the largest contribution arising from the second-order Zeeman interactions.[45] Thus, only a single spin state is populated in this temperature range. In conclusion, on the basis of NMR results, the alkyliron (or aryliron) porphyrins are always in the low-spin state in solution.

Effect of the Porphyrinic Macrocycle. Dependence on the nature of the equatorial ligands has been previously reported.[58] In solution, at room temperature no electronic spin change is observed with a change in the nature of the porphyrin macrocycle by NMR spectroscopy. On the contrary, in frozen toluene solution at 115 K, ESR data prove unambiguously that a basic porphyrin ligand such as T(p-Et_2N)PP leads preferentially to a high-spin complex and that the (β-CN)$_4$TPP electron-withdrawing ligand gives a pure low-spin state for the aryliron(III) species. In the case of unsubstituted TPP and OEP porphyrins two spin states are observed. This result shows that the spin state is critically dependent on the basicity of the macrocycle: the metal–ligand bond strength decreases when the metal electron density of the electron donor properties of the macrocycle increases. Then it is possible to order the porphyrin ligand vs the increasing basicity: (β-CN)$_4$TPP < TPP ≃ T(p-Me)PP ≃ T(m-Me)PP < OEP < T(p-Et_2N)PP. The ESR results show the existence of two spin states according to the nature of the alkyl or aryl ligand and the macrocycle in frozen toluene solution, the spin mixture shift depending on the axial ligand strength for a given macrocycle.

The ESR temperature study (Figure 4) suggests that the spin mixture is static, and the critical decreasing of the $g_\perp$ signal at low temperature may be explained by the thermal dependence

(50) Eaton, S. S.; Eaton, G. R. *Inorg. Chem.* **1980**, *19*, 1095.
(51) Drago, R. S. *Physical Methods in Chemistry*; W. B. Saunders: Philadelphia, 1977; Chapter 11.
(52) Mitra, S. In *Iron Porphyrins*; Lever, A. B. P., Gray, H. B., Eds.; Addison-Wesley: Reading, MA, 1983; Part II, Chapter 1.
(53) Hill, H. A.; Skyte, P. D.; Buchler, J. W.; Lueken, H.; Tonn, M.; Gregson, A. K.; Pellizer, G. *J. Chem. Soc., Chem. Commun.* **1979**, 151.
(54) Gunter, M. J.; Mc Laughlin, G. M.; Berry, K. J.; Murray, K. S.; Irving, M.; Clark, P. E. *Inorg. Chem.* **1984**, *23*, 283.
(55) Geiger, D. K.; Lee, Y. J.; Scheidt, W. R. *J. Am. Chem. Soc.* **1984**, *106*, 6339.
(56) Geiger, D. K.; Chunplang, V.; Scheidt, W. R. *Inorg. Chem.* **1985**, *24*, 4736.
(57) Reed, C. A. In *Electrochemical and Spectroelectrochemical Studies of Biological Redox Components*; Kadish, K. M., Ed.; American Chemical Society: Washington, DC, 1982; Chapter 15.
(58) Geiger, D. K.; Scheidt, W. R. *Inorg. Chem.* **1984**, *23*, 1970.

of the Kramer's doublet population.[47] But these ESR results are not in good agreement with those of the NMR study. Indeed, no high-spin species is detected in toluene solution in the range 193–333 K by NMR spectroscopy. For a given sample, only the low-spin state is observed by NMR, whereas the two spin states can be detected by ESR according to the nature of the axial alkyl or aryl group and the equatorial ligand. A chemical change of the iron complexes cannot be excluded, but no decay is observed after several temperature cycles. Other parameters such as matrix effects must be involved.

Solvent Effects. Figure 5b illustrates the ESR spectrum of (OEP)Fe(CH_3) recorded at 115 K in frozen carbon disulfide solution. A large spin state shift toward the low-spin state is observed. The carbon disulfide molecules could coordinate the metal center. In fact, ^{1}H NMR spectra did not show any change in carbon disulfide solution, and after recrystallization in the same solvent, no supplementary ligand has been detected by IR spectroscopy. Moreover, the coordination scheme of σ-alkyliron(III) (or σ-aryliron(III)) porphyrins has been studied by resonance Raman spectroscopy.[59] The spectroscopic data show that the iron atom is always pentacoordinated whatever the solvent (toluene, benzene, or carbon disulfide), the temperature (between 163 and 293 K), or the nature of the axial (methyl or phenyl group) or equatorial (TPP or OEP) ligands. All these studies prove that carbon disulfide acts as solvent and a glassy solvent matrix induces iron spin state change.

Solid Measurements. The isomeric shift relative to metal iron of high-spin iron(III) porphyrin is close to 0.4 mm s^{-1}. For intermediate-spin derivatives ($S = {}^3/_2$) a quadrupole splitting higher than 3 mm s^{-1} is observed whereas for the low-spin complexes ($S = {}^1/_2$), the corresponding values is 2.2 mm s^{-1}.[60-62] Our Mössbauer data prove unambiguously that perfluoroaryl porphyrins are in a high-spin state ($S = {}^5/_2$). On the contrary, the Mössbauer data of (alkyl or aryl)ferriporphyrins are similar to those of low-spin species (Tables VII and VIII and Figures 7 and 8). For the (OEP)Fe(C_6H_5) complex, the quadrupolar splitting is almost constant in the range of investigated temperatures, and the isomeric shift decreases when the temperature increases. This decreasing is not rigorously linear, and a linear regression gives a slope $d\delta/dT = -3.7 \times 10^{-4}$ mm s^{-1} K^{-1}.

At 85 K the quadrupolar doublet is dissymetric, the high-energy line width increases, and the low-energy band decreases. Texture effects cannot be invoked because this dissymetry disappears at high temperature. The molecular geometry of the ferriporphyrin complexes could explain this phenomena. Indeed, the coordination of the σ-bonded complexes are close to those of HbN_3 and HbCN for which similar dissymetry appears.[63] At 85 K the spin–lattice relaxation speed is too high, and no magnetic coupling is observed. However, the low-temperature spectra of (OEP)Fe(C_6H_5) reveal a very weak absorption close to 0.3 mm s^{-1} which can be due to the presence of high-spin iron(III) species (see Figures 7 and 8). We cannot make a conclusion unambiguously, but it is remarkable to note that the magnetic moment values of the (P)Fe[R(Ar)] complexes are slightly higher than those of regular low-spin iron(III) porphyrins. Thus, it means that the high-spin species amount is very low in spite of ESR signals intensity.

As seen in Figure 6, the ESR spectrum strictly depends on the method of sample preparation. The grinding is a surface area effect implying that the spin mixture shift toward the high-spin state is small. Microcrystal grinding leads to modification of the interaction between each paramagnet, and the high-spin species must be essentially localized in surface. We can reasonably expect that the high-spin species results from the modification of the molecular structure due to the out-of-macrocycle plane metal displacement. Thus, the high values of effective magnetic moment can be interpreted by a strong orbital contribution and the presence of complexes in both spin states ($S = {}^1/_2$ and $S = {}^5/_2$). This interpretation agrees with the above results in frozen solution where the intermolecular interactions vary with the nature of solvent matrice.

But according to the Mössbauer results, the number of high spin sites is very low and the (alkyl or aryl)ferriporphyrins are preferentially in low spin state. The existence of some high-spin sites proves that the two spin states are very close in energy.

Conclusion

Some ligand spin state stereochemistry relations can be deduced from this study. The (alkyl or aryl)ferriporphyrins show an unusual magnetic behavior since these species are either in low-spin or high-spin states or in low-spin state with some high-spin sites. This behavior depends on the nature of axial and equatorial ligands, and the spin state is dependent on several physical parameters. The study of the magnetic properties of σ-bonded iron–carbon porphyrins allows us to predict the molecular geometry. In particular the electron-donor or -withdrawing character of the axial and porphyrin ligands modifies the iron distance from the mean plane of the porphyrin. This distance decreases with the spin multiplicity in the case of strong field axial ligands. For such compounds the pentacoordination scheme tends to keep the iron atom slightly out of the plane of the four nitrogen atoms. Recently, two crystal structures of (TPP)Fe(C_6H_5) and (TAP)Fe(SH) confirmed this assumption.[34,64] For (TPP)Fe(C_6H_5) the iron atom lies only at 0.17 Å from the four nitrogen plane. The spin state change ($S = {}^1/_2 \rightarrow S = {}^5/_2$) can be interpreted by expansion of the central hole and the lengthening of the iron–carbon axial bond.

On the basis of g factors we have calculated the rhombicity V/Δ and the tetragonal distorsion Δ/λ for all the studied complexes (Tables IV–VI). The values of V/Δ (pure geometric factor) show that for most of the complexes the distorsion in the xy plane is more important that the lengthening along the z axis ($V/\Delta > 0.66$). This unusual property is attributable to the absence of the second axial ligand. Moreover, we can compare the different derivatives taking into account the π-electronic transfer since a π-donor axial ligand induces an increasing of Δ/λ and a π-acceptor axial ligand a decreasing. For (TPP)Fe(C_6H_5) in toluene, the value of Δ/λ is 4.14 whereas, for (TPP)Fe(p-MeC_6H_4), this term is 5.98. This example shows the important decrease of the π-acceptor effect of the aryl group, and this property could be postulated only on the basis of NMR data. The calculations of rhombicity of the V/Δ crystal field for the same complex under different conditions (in solution toluene or carbon disulfide solution; solid diluted in magnesium sulfate) lead to very close values. For (TPP)Fe(C_6H_5), V/Δ varies from 0.81 to 0.86 (Tables IV–VI). This confirms that there is no structural change—i.e. solvent coordination—of the complexes in various matrices.

Registry No. (OEP)Fe(n-C_4H_9), 79198-01-9; (OEP)Fe(CH_3), 79197-83-4; (OEP)Fe(C_6H_5), 83614-06-6; (OEP)Fe(p-MeC_6H_4), 83614-08-8; (TPP)Fe(n-C_4H_9), 79198-00-8; (TPP)Fe(Me), 79197-95-8; (TPP)Fe(C_6H_5), 70936-44-6; (TPP)Fe(p-MeC_6H_4), 87621-56-5; [T(p-Et_2N)PP]Fe(C_6H_5), 96482-35-8; [(β-CN)$_4$TPP]Fe(C_6H_5), 96502-39-5; [T(m-Me)PP]Fe(n-C_4H_9), 111410-28-7; [T(m-Me)PP]Fe(CH_3), 87607-81-6; [T(m-Me)PP]Fe(C_6H_5), 87607-83-8; [T(p-Me)PP]Fe(n-C_4H_9), 111410-29-8; [T(p-Me)PP]Fe(Me), 87607-82-7; [T(p-Me)PP]-Fe(C_6H_5), 87607-84-9; (OEP)Fe(C_6F_4H), 111410-30-1; (OEP)Fe(C_6F_5), 96502-36-2; (TPP)Fe(C_6F_4H), 111410-33-4; (TPP)Fe(C_6F_5), 96502-37-3; [T(m-Me)PP]Fe(C_6F_4H), 111410-31-2; [T(m-Me)PP]Fe(C_6F_5), 96502-38-4; [T(p-Me)PP]Fe(C_6F_4H), 111410-32-3; [T(p-Me)PP]Fe-(C_6F_5), 96532-02-4; (TPP)FeCl, 16456-81-8; (TPP)Fe(Im)$_2$Cl, 25442-52-8; (OEP)Fe(ClO_4), 50540-30-2.

(59) Tabard, A.; Lagrange, G.; Guilard, R.; Jouan, M.; Dao, N. Q. *J. Organomet. Chem.* **1986**, *308*, 335.
(60) Dolphin, D. H.; Sams, J. R.; Tsin, T. B.; Wong, K. L. *J. Am. Chem. Soc.* **1978**, *100*, 1711.
(61) Dolphin, D. H.; Sams, J. R.; Tsin, T. B. *Inorg. Chem.* **1977**, *16*, 711.
(62) Epstein, L. M.; Straub, D. K.; Maricondi, C. *Inorg. Chem.* **1967**, *6*, 1720.
(63) Lang, G. *J. Appl. Phys.* **1967**, *38*, 915.
(64) English, D. R.; Hendrickson, D. N.; Suslick, K. S.; Eigenbrot, C. W.; Scheidt, W. R. *J. Am. Chem. Soc.* **1984**, *106*, 7258.